# AIAA 2003–0185
# Aerodynamically Controlled Expansion Nozzle for STOVL Aircraft

D.A. Terrier
Lockheed Martin Aeronautics Company, Fort Worth, TX
and
F.K. Lu
University of Texas at Arlington, Arlington, TX

**41st Aerospace Sciences Meeting & Exhibit**
6–9 January 2003
Reno, Nevada

# Aerodynamically Controlled Expansion Nozzle for STOVL Aircraft

Douglas A. Terrier*

*Lockheed Martin Aeronautics Company, Fort Worth, Texas 76101*

Frank K. Lu†

*University of Texas at Arlington, Arlington, Texas 76019*

**An aerodynamically controlled expansion propulsion nozzle that improves hover thrust performance by 2.5 percent in a short take off and vertical landing aircraft was developed. The nozzle concept employs a step in the nozzle internal contour that interacts with the boundary layer to induce flow separation in the divergent section, thereby relieving over-expansion losses during hover. This study specifies design parameters for a passive boundary layer control step for application on the F-35 Joint Strike Fighter. In addition, parametric performance predictions demonstrate that the step concept can be applied to overcome undesirable over-expansion in generalized supersonic nozzle flows.**

## Nomenclature

| | |
|---|---|
| $A$ | cross-sectional area |
| $C_{fg}$ | gross thrust coefficient |
| $F$ | thrust |
| $L_f$ | flap length = 41 cm |
| $\dot{m}$ | mass flux |
| NPR | nozzle pressure ratio |
| STOVL | short take-off and vertical landing |

subscripts

| | |
|---|---|
| $s$ | slot or step |
| $t$ | total |
| 8 | nozzle throat |
| 9 | nozzle exit |

## Introduction

THE development of fixed wing STOVL aircraft presents a conundrum to engineers attempting to exploit the aircraft's military advantages. A fundamental technical challenge lies with the propulsion system, which must be efficient for high-speed flight and during hover. At the same time, the STOVL propulsion system must address the mechanical complexity required for converting the thrust stream from horizontal to vertical.

Amongst the latest generation of STOVL aircraft is the F-35 Joint Strike Fighter (JSF). The JSF propulsion system utilizes the Pratt and Whitney F-119 turbofan engine that is well matched for transonic fighter operation. It provides good fuel efficiency at cruise, and high thrust in augmented mode for transonic acceleration and supersonic operation. Specifically, the JSF STOVL propulsion system operates over a wide range of conditions. Due to the emphasis on weight savings and affordability in the JSF program, it is highly desirable to minimize mechanical complexity.

A situation where the desire for mechanical simplicity and high propulsion performance are in direct conflict is the exhaust system. The exhaust flow conditions in hover are dramatically different from those in transonic acceleration, yet the nozzle provides the same flow-path in both cases (Fig. 1). Specifically, the nozzle mechanical arrangement is scheduled to provide an internal expansion ratio of 1.3 to give good performance for the critical transonic acceleration portion of the mission. The nozzle expansion ratio of 1.3 is also presented in the hover case. But this situation produces over-expansion of the flow, resulting in significant thrust loss. If the nozzle expansion ratio was reduced to 1.1, however, the gross thrust coefficient at hover will increase from approximately 0.92 to at least 0.96.[1] Table 1 summarizes some of the nozzle parameters at three mission points.

This investigation proposes to develop an aerodynamic solution that mitigates thrust losses due to over-expansion in the JSF nozzle at the hover condition. A preliminary examination of candidate solutions was conducted, of which one was selected. This solution was then studied primarily using an axisymmetric Navier–Stokes computational simulation to analyze a parametric range of nozzle geometry and operating conditions. The analysis was validated by sub-scale experiments.

*Manager. Member AIAA.

†Professor, Mechanical and Aerospace Engineering Department, and Director, Aerodynamics Research Center. Associate Fellow AIAA.

## Candidate Techniques

There are a number of possible techniques that provide nozzle expansion control through aerodynamic rather than purely mechanical means. Some of the pertinent approaches that make use of aerodynamic area control in nozzles to relieve over-expansion loss are briefly described. These techniques range from geometric tailoring of the divergent flaps to admit ambient air to the use of secondary air systems. In all cases examined, the underlying principle is fundamentally the same. The intent is to displace the primary airflow away from the divergent flap to achieve an effectively smaller nozzle expansion area ratio. The techniques differ primarily in the mechanism used to displace the primary flow.

One geometric tailoring approach is the use of longitudinal slots or vents in the divergent flaps to admit secondary air.[2,3] The vented flap approach provides performance improvement at over-expanded conditions but, conversely, suffers performance losses at under-expanded conditions. By definition, the vented flap design cannot provide a continuous load path around the circumference of the nozzle, resulting in an inefficient pressure vessel. The vented flap design also requires that the nozzle segments be cantilevered, which results in large actuation forces. For these reasons, the vented flap approach tends to be heavy relative to conventional convergent-divergent (C-D) nozzles and is not an attractive solution for a STOVL aircraft where weight is at a premium.

Secondary flows can also be used for nozzle over-expansion relief. Specifically, these use ejector and injector concepts. These techniques involve a secondary flow stream usually introduced through a slot at or downstream of the nozzle throat. This secondary flow displaces the primary nozzle flow from the nozzle wall, resulting in a lower effective expansion area.

For this discussion, the difference between ejectors and injectors lies in the pressure of the secondary stream. Injectors use a secondary stream at high pressure that is injected into the primary stream. In the case of ejectors, the secondary stream is usually at ambient pressure and is passively entrained by the viscous interaction of the primary flow. Both of these approaches have shown promise in managing the aerodynamics of the expanding flow in the divergent section of nozzles.

Injectors have been in use for decades in rocket nozzles, primarily as a means of vectoring thrust. A high-pressure secondary flow is injected asymmetrically in the divergent section of the nozzle to displace the primary flow from the wall and produce a non-axial thrust vector. This approach achieves thrust vectoring without the complexity of a mechanically vectored nozzle. Recent technology advances have created a strong interest in fixed geometry nozzles for turbofan engines. As a result, considerable effort has been expended recently toward developing aerodynamic methods for controlling nozzle throat and exit areas as well as achieving thrust vectoring.

Among the techniques being considered for aerodynamic nozzle control is secondary flow injection. Recent studies have shown that steady-state injection flow systems can be effective in providing nozzle area control and vectoring. Miller et al.[4] showed that injector effectiveness is a function of injector geometry and axial location. However, the high-pressure secondary flow must be obtained from costly engine bleed air or from an auxiliary pump or turbine. The injector must be routed through high-pressure ducting from the source to the nozzle. In addition, a complex system of control valves is required to modulate the injector flow.

Some investigators have suggested that higher injector effectiveness can be achieved with pulsed rather than steady flow.[5] The increased effectiveness comes at the cost of additional complexity in high-frequency valves and control systems. In the JSF application, the additional cost and complexity of injector systems with their high-pressure supply, valves, and control systems must be carefully traded against the performance benefit.

A passive aerodynamic approach to nozzle expansion control is found in ejector nozzles. Ejectors have been in use since the 1960's in military aircraft such as the F-4 and the F-111. The ejectors in these designs serve a dual purpose. These aircraft engines had limited $A_9$ control, being designed with high nozzle area ratio to provide good performance at supersonic, high NPR conditions. Thus, analogous to the JSF hover case, these aircraft suffered over-expansion loss at low speeds and reduced power settings. Ejectors were used to improve thrust efficiency at these off-design conditions. In addition, these early jet aircraft used pure turbojets, which operated at high temperatures and did not have the benefit of a secondary fan stream for cooling. Cool secondary air was directed through the engine bay to cool the structure around the engine and to purge combustible gases.

A wealth of data can be found in ejector studies dating back to the 1950s, prior to the introduction of variable $A_9$ nozzles when ejector nozzles were the primary means of expansion control. Ejector studies have traditionally focused on two separate aspects of performance.[6] The first aspect is the air handling or pumping characteristics that describe the effectiveness of the system in entraining secondary flow. A parametric investigation by Greathouse and Beal[7] provides one of the most comprehensive single database on ejector air handling and thrust performance.

An example of Greathouse and Beal's results is shown in Fig. 2. The figure shows that $C_{fg}$ generally increases

with increasing secondary flow, particularly at low NPR where severe over-expansion is present. The data clearly show the effectiveness of ejectors at reducing over-expansion losses from the perspective of nozzle efficiency. But, that component-level improvement does not necessarily translate to a system-level benefit. The JSF is a highly compact design, making it difficult to introduce secondary flow-paths. In addition, external shaping and surface treatments make it highly undesirable to introduce secondary inlets. In the JSF application, the additional cost and complexity of ejectors must be carefully traded against the potential performance gain.

The results of Ref. 7, however, provide important clues to a previously unexplored approach to relieving over-expansion loss. The data for no secondary flow show an interesting trend at low NPR. In all cases, $C_{fg}$ falls off rapidly with decreasing NPR in the over-expanded region. However, at a critical NPR, $C_{fg}$ abruptly returns to a relatively high value. This phenomenon results in a $C_{fg}$ at low NPR that is higher than would be predicted by first-order analysis.[1] When there is no secondary flow through the slot just downstream of the nozzle throat, the configuration is essentially an aft-facing step. It is postulated that this step interacts with the boundary layer, causing the flow to separate from the divergent flap, relieving the over-expansion loss through an aerodynamic tailoring effect.

This step could therefore provide a simple and inexpensive alternative to injector or ejector nozzle systems for relieving the over-expansion loss in the JSF nozzle at hover. The resulting flow in the region downstream of the step would be separated from the divergent flap and bounded by a supersonic free shear layer. The behavior of such separated, supersonic flows downstream of an aft facing was examined by Abu-Hijleh and Samimy.[8] That study showed that, depending on the nozzle pressure ratio, the flow may remain separated to the nozzle exit or re-attach at some point downstream on the divergent flap. Further, the behavior of the downstream flow is influenced by the specific shape of the step.[9]

The separation phenomenon is often neglected in ejector thrust studies since it is not present under normal operation with the presence of secondary flow. The phenomenon is, however, evident in ejector air handling characteristics. Kochendorfer and Roussou[10] describe the abrupt change in divergent section pressures and ejector air handling characteristics that occur at this condition. They refer to the NPR at which the performance changes abruptly as the "break-off" pressure ratio, apparently in recognition of the divergent flap separation phenomenon.

***First-Order Analysis***

The data from several ejector configurations in the literature were compiled to provide a database for examining the interaction of the ejector slot when no secondary flow is present. Figure 3 shows a plot of the NPR at separation versus secondary step size. The separation NPR is defined by the minima in the over-expanded region of the $C_{fg}$ curves. The slot size is presented as a normalized value using the ratio of flow-path cross-sectional area at the slot to the nozzle throat area ($A_s/A_8$). This plot shows the minimum slot (or step) size required to assure boundary layer separation at a given NPR. From Fig. 3, for the JSF hover condition with NPR = 2, the minimum slot area ratio to achieve separation is expected to be $A_s/A_8$ = 1.1.

While the step induces boundary layer separation at low NPR and increases thrust, the drag on the step will produce a thrust loss at the design NPR. Luffy and Hamed's[11] study on ejector nozzle slots showed that the pressure acting on the aft facing step is a function of the specific local geometry, and is on the order of $0.2p_t$, producing a step drag. The magnitude of the thrust loss at peak NPR resulting from step drag can be estimated from empirical data by comparing peak $C_{fg}$ for ejector nozzles with $\dot{m}_s/\dot{m}_p = 0$ with that predicted for similar non-ejector nozzles using a quasi one-dimensional analysis.[1] This comparison using data from Ref. 7 predicts that, at a minimum effective step size of $A_s/A_8$ = 1.1 for the JSF hover condition, $C_{fg}$ is reduced by 0.5 percent at the design NPR. It can be concluded that a simple mechanical step can induce boundary layer separation and provide a method for improving over-expansion loss at low NPR.

Based on techniques described in the literature, and the preliminary analysis described above, three candidate approaches to solving the JSF over-expansion thrust loss were identified, namely, a boundary layer control step, an ejector nozzle and injector nozzle. Moreover, three different implementations of the step were considered. These are a simple fixed step, a mechanically variable step, and a step utilizing a micro electro-mechanical system (MEMS) for actuation. Of these, the fixed step is potentially the simplest, but will result in performance loss at the design condition. The variable step or MEMS solves this problem by allowing the step to be retracted when the nozzle is operating on-design, but require more complex and costly actuation and control systems.

The ejector concept was considered with two different sources of secondary air. The first is a main inlet off-take and the second is a dedicated secondary inlet on the external surface of the aircraft. Both of these present unique integration problems. The main inlet off-take requires ducting through the aircraft to carry air to the nozzle. Small ducts create significant secondary air pressure drop while large ducts are difficult to integrate. A secondary inlet could be provided near the nozzle avoiding duct losses; however, the additional orifice presents may compromise the aircraft's radar signature.

Three injector configurations were considered: a steady-state injector located at the throat, one downstream on the flap, and a pulsed-injection concept. The throat slot location is easiest to implement but studies show that a downstream location may be more effective. Pulsed injector systems require additional complexity in valves and control systems. All three injector systems offer potentially high effectiveness but this must be traded against the additional system complexity, weight and cost inherent in the high-pressure flow supply, ducting, valves and control systems.

The eight approaches were subjected to a qualitative screening process. For the JSF application, the primary figure of merit in any design decision is total lifecycle cost, which consists of development cost, procurement cost, and operations and support cost. Other figures of merit are weight, technical risk, system integration impact, and survivability impact. The outcome of this qualitative analysis is that a mechanical step provided the most promising approach to solving the JSF over-expansion loss. This investigation therefore proceeded to an in-depth numerical analysis of the step configuration to understand the flow behavior, develop a viable design, and validate it through testing. The technique for overcoming the over-expansion loss is known as an *aerodynamically controlled expansion* (ACE) nozzle.

## CFD Analysis

A parametric numerical study was performed for eight nozzle configurations at NPR = 2–8, nozzle area ratios of 1.1–1.5 and step area ratios $A_s/A_8$ of 1–1.2, for a total of 33 cases. This configuration matrix fully covers the potential design space for the JSF application. The results of the CFD analysis therefore provide a generic design database in addition to predicting the performance of individual step configurations. The results of the CFD analysis substantiated the effectiveness of the step, defined a preferred configuration and provided design guidance for scale model validation testing.

### *Falcon Code Description*

The numerical study used the Falcon CFD code developed at Lockheed Martin Aeronautics Company from the early 1980s. Over the last two decades, the code has undergone continuous development to extend its capability. The code has been validated against experiments of complex flow phenomena pertinent to aerospace systems. Falcon was selected for the present study particularly because of its demonstrated capability to accurately solve transonic flows dominated by viscous phenomena.

Falcon is a Reynolds-averaged Navier–Stokes solver that uses a finite-volume approach on a multiple block, structured grid. The finite-volume technique allows the code to achieve better conservation qualities than comparable finite-difference codes. Two implicit solvers, the strongly implicit procedure and the symmetric successive over relaxation are available. To reduce turnaround time, Falcon uses a block parallel capability using either message passing interface or parallel virtual machine message passing utilities.

The Falcon code includes the two-equation $k$–$\ell$ and $k$–$k\ell$ turbulence models, and a large eddy simulation model for accurate turbulence calculations and a wall-layer model (or wall function) to reduce the number of points required for accurate boundary layer calculations. The code also includes the capability to solve very low speed and mixed speed flows using a technique known as low speed preconditioning. The preconditioning is effective at all subsonic Mach numbers and provides significant improvements in efficiency at Mach numbers below 0.3.

Other code features include the ability to run two-, three- and axi-symmetric problems; a mature time-accurate capability; third-order spatial accuracy; an implicit vortex generator model; an overset grid capability; and a variety of boundary condition types. In order to solve geometrically complex problems, the code includes capability for internal boundary conditions and multiple blocks of grid. Boundary conditions can be set along any grid surface or line in the grid.

Three types of interfaces between multiple blocks of grid are currently available in Falcon. The first assumes the grids match at the boundary point-for-point. The second is called non-point-to-point matched and only requires that an extrapolated grid point can be found in some other block. The third type is similar to the matched interfaces except that the interface data is filtered through some type of transfer function before being applied to the opposite interface patch.

A number of user-oriented features have also been built in to the Falcon code. A preprocessor program, known as T3d, translates boundary condition (BC) specifications from the Gridgen code to produce a Falcon BC file. It also allows the user to easily combine or divide 3-D grids while maintaining interface connectivity and boundary condition specifications. For restart files, grids and bc specifications, the code uses an enhanced, self-describing, machine independent file system.

Other user-oriented features include the capability to pick the flow output parameters from a menu of choices and then output that data to the standard output file or to a file or files specified by the user. A number of integrated quantities can also be computed on the fly and written to a file specified by the user. In this way the user can monitor the convergence of lift, drag, mass flow, thrust, pressure recovery, amongst others.

### *CFD Analysis Matrix and Boundary Conditions*

In this analysis, Falcon was run in the axi-symmetric mode with a grid consisting of approximately 90 points in the axial direction and 40 points in the radial direction for a total of about 3,600 grid points. The configurations simulate variations on the JSF nozzle in the hover or after-burning mode with $A_8$ = 0.484 m$^2$. Three nozzle expansion ratios of $A_9/A_8$ = 1.1, 1.3 and 1.5 were examined, representing the range of expansion ratios that could practically be considered for the JSF application. An example of a typical grid structure for the $A_9/A_8$ = 1.3 baseline (no step) case is shown in Fig. 4. Grid details in the region of the step are shown for the $A_9/A_8$ = 1.3, $A_s/A_8$ = 1.1 case in Fig. 5.

For the $A_9/A_8$ = 1.1 case, a baseline configuration and a slot size of $A_s/A_8$ = 1.1 were run. For the $A_9/A_8$ = 1.3 and $A_9/A_8$ = 1.5 cases, a baseline configuration, and $A_s/A_8$ = 1.1 and 1.2 were run. All cases were run at full-scale geometry with a representative engine exhaust total temperature of 780 K.

Inflow total pressure was specified to simulate hover at NPR = 2.0 to supersonic after-burning acceleration at NPR = 8.0. The exit boundary condition was specified at sea level standard atmospheric conditions of $P$ = 101.3 kPa and $T$ = 294 K. In order to capture the interaction of the external flow-field, the grids extend to the region outside the nozzle. External flow velocity was specified at Mach 0.05.

## Numerical Results

### *Baseline Configuration*

Results of the CFD analysis for the baseline configuration at the hover condition are presented in Fig. 6. Velocity vectors are shown as scaled arrows. Several flow features are evident in a close examination of this plot. The flow is seen to accelerate through a Prandtl–Meyer expansion from a sonic condition approaching the throat to high supersonic speed as it continues into the divergent section. The initial Prandtl–Meyer fan just downstream of the throat is governed by the divergent flap angle. Further flow expansion occurs in the complex flow region downstream due to reflected waves.

Also shown in Fig. 6 is the pressure along the nozzle surface. The flow is highly over-expanded, producing sub-ambient pressures along almost the entire extent of the divergent flap. This low-pressure region acting on the aft-facing part of the flap produces a significant drag that is the source of the thrust loss at hover. Near the trailing edge, the adverse pressure gradient due to the influence of the ambient pressure results in local boundary layer separation. In the separated region, the flow recovers to the ambient pressure. This recovery actually helps to reduce the over-expansion drag.

It should be noted that this is an unusual situation in which boundary layer separation may actually be desirable for drag reduction. In this case the low pressures on the divergent flap resulting from over-expansion produce more drag than a separated flow. It is intuitively obvious from the baseline results that a configuration that promotes more extensive separation along the divergent flap will yield less drag and therefore higher thrust. This reveals the essential principle behind the step configurations developed in this study. Specifically, the step promotes boundary layer separation thereby reducing drag on the divergent flap.

The CFD results for the baseline configuration at NPR = 6 representing the transonic acceleration, after-burning point are shown in Fig. 7. In this high NPR case, the flow remains at higher than ambient pressure as it expands through the divergent section of the nozzle. In contrast to the hover case, the divergent flap yields positive pressure resulting in additional thrust. This illustrates the physical reason why this relatively large area ratio of $A_9/A_8$ = 1.3 is required to exploit the thrust potential of the flow at this condition.

The computed values of thrust coefficient for the baseline nozzle are compared in Fig. 8 with experimental results.[1] The numerical predictions show excellent agreement with the test data and illustrate the over-expansion thrust loss at low NPR. The accuracy of the numerical method can be seen by the consistency between the numerical and experimental data. Figure 8 shows other numerical results that will be discussed later.

### $A_s/A_8$ = 1.1 *Step Configuration*

The numerical results for $A_9/A_8$ = 1.3, with a slot area ratio of $A_s/A_8$ = 1.1 at the hover condition of NPR = 2 are shown in Fig. 9. In this case, boundary layer separation is induced by the step and the flow is not attached to the nozzle walls. The Prandtl–Meyer expansion at the throat and over-expansion downstream are not as severe as in the baseline case. The net effect is that pressures on the divergent flap are higher than for the baseline case.

Between the divergent flap and the nozzle flow is a region of separated flow. Close examination of Fig. 9 reveals the presence of an inflow from the external flow-field into this cavity and a region of re-circulation adjacent to the primary flow slip line. The entrainment in this region produces pressures that are below ambient, but still higher than the baseline case. The figure also shows the higher divergent flap pressures compared to the baseline (Fig. 6), which yields a reduced drag.

The result for the $A_9/A_8$ = 1.3, $A_s/A_8$ = 1.1 case at transonic acceleration with NPR = 6 is shown in Fig. 10. In this case, boundary-layer separation is initially induced

by the step causing a separated region immediately downstream of the throat. Unlike the hover case, the favorable pressure gradient for this case causes the flow to immediately re-attach to the divergent flap. Above-ambient pressures are experienced along the remainder of the divergent flap giving good thrust performance.

The performance of the $A_s/A_8$ = 1.1 configuration was also examined at several other NPR. Gross thrust coefficients for the $A_s/A_8$ = 1.1 configuration are compared with that of the baseline in Fig. 8. The figure shows a potential for improvement in hover $C_{fg}$ of about 2.5 percent with the $A_s/A_8$ = 1.1 configuration relative to the baseline. This translates into the potential for a dramatic increase of about 4 kN in aircraft payload.

***Effect of Step Configuration and Nozzle Area Ratio***

The effect of different step sizes was also investigated. Figures 11 and 12 show results for the $A_9/A_8$ = 1.3 configuration with the larger slot size of $A_s/A_8$ = 1.2 at NPR = 2 and 6 respectively. At NPR = 2, the large step produces separation, giving results similar to the $A_s/A_8$ = 1.1 case. At the transonic acceleration condition at NPR = 6, the flow reattaches just downstream of the step as in the $A_s/A_8$ = 1.1 case, but low pressures in the separated region act on the larger aft facing step producing a higher thrust loss of about one percent.

Figures 13 and 14 show results for the baseline nozzle geometry with a larger nozzle area ratio of $A_9/A_8$ = 1.5 at NPR = 2 and 6 respectively. The results are similar to the baseline nozzle at $A_9/A_8$ = 1.3 but, due to the larger area ratio, show lower divergent section pressures that exacerbate the over-expansion loss at hover. Note that the highly over-expanded flow exhibits a large region of separated flow as it approaches the trailing edge. This spontaneous boundary layer separation is due to the adverse pressure gradient imposed by ambient pressure.

The results for the larger area ratio of $A_9/A_8$ = 1.5 and with a step of $A_s/A_8$ = 1.1 are shown in Figs. 15 and 16 for NPR = 2 and 6 respectively. Compared with the baseline nozzle (Fig. 13), Fig. 15 illustrates the effectiveness of the step in inducing separation and relieving over-expansion at the hover condition. At the transonic acceleration condition with NPR = 6 shown in Fig. 16, the reattachment and step drag phenomena are again evident. The $A_9/A_8$ = 1.5 configuration was also run at several NPR values and with a step size of $A_s/A_8$ = 1.1.

Numerical results for the baseline nozzle geometry with a modified $A_9/A_8$ = 1.1 indicate higher divergent section pressures than the baseline nozzle with $A_9/A_8$ = 1.3 as a result of the smaller area ratio. In the hover case at NPR = 2, the $A_9/A_8$ =1.1 configuration yields a $C_{fg}$ improvement of approximately 4 percent relative to the baseline nozzle with $A_9/A_8$ = 1.3. In contrast, the NPR = 6 case shows significant under-expansion with pressures remaining higher than ambient at the trailing edge of the divergent flap. This results in a thrust loss at the critical transonic acceleration condition of NPR > 6 and illustrates why it is not practical to re-schedule the nozzle to $A_9/A_8$ = 1.1 to improve performance at hover. Numerical results for a modified $A_9/A_8$ = 1.1 with a step size of $A_s/A_8$ = 1.1 at NPR =2 show separation induced by the step. However at this small $A_9/A_8$ = 1.1, over-expansion losses are small and any performance gains resulting from separation are negated by the step drag penalty.

***Summary of Numerical Analysis***

The $C_{fg}$ values from the CFD analysis are summarized in Fig. 17. The summary data are re-plotted in Fig. 18. Figure 18a shows that separation occurs at higher NPR with increasing $_{As}/A_8$ or $A_9/A_8$ while Fig. 18b shows the relationship between the change in $C_{fg}$ versus step size and NPR. The results show that the step boundary-layer control configuration can provide improvements in the hover performance of the JSF propulsion system. The results indicate that the $A_9/A_8$ = 1.3 and $A_s/A_8$ = 1.1 configuration can yield a 2.5 percent improvement in $C_{fg}$ relative to the baseline nozzle. For this configuration, a minor thrust loss of approximately 0.5 percent in $C_{fg}$ is predicted at the transonic acceleration condition.

The results also illustrate that reducing the scheduled nozzle area ratio to $A_9/A_8$ = 1.1 is not a practical way of improving hover thrust because this low $A_9/A_8$ produces an under-expanded condition at transonic acceleration that results in an unacceptable loss. The numerical results show that the small step ratio of $A_s/A_8$ = 1.1 is sufficient to induce boundary layer separation at the JSF hover condition. Increasing the step size adversely affects performance at higher NPR conditions.

Increasing $A_s/A_8$ results in separation occurring at higher NPR. However, increasing step size above the minimum required for a given application is not desirable because of step drag that causes thrust loss at conditions other than hover. Increasing $A_9/A_8$ also results in separation occurring at a higher NPR. This result is to be expected because increasing $A_9/A_8$ leads to more sever over-expansion. Lower pressure in the divergent nozzle makes the flow more prone to separation.

**Mechanical Implementation**

The numerical analysis and subscale test results (the latter not reported here) showed that the step boundary layer control concept is effective in improving hover thrust performance by approximately 2.5 percent. However, this benefit can only be realized if the concept can be practically implemented on the JSF nozzle design. A preliminary mechanical design study was conducted to evaluate the feasibility of incorporating the step concept

in the JSF nozzle design. The design study followed two ground rules. First, the step design must be simple, lightweight and low cost. Second, the implementation scheme must be self-contained, resulting in no mechanical interference, functional interface or modification to other aircraft systems.

Two mechanical implementation schemes were examined. Both approaches provide a simple mechanism for providing the step geometry in the flow-path as desired at the hover condition, but presenting no step and therefore no step drag at cruise. The first scheme involves a modification to the trailing edge of the exhaust duct liner at the nozzle throat as shown in Fig. 19. The second scheme utilizes an offset hinge mechanism at the nozzle throat as shown in Fig. 20. A conceptual mechanical design was developed to verify the mechanical feasibility and assess integration impacts. Based on the conceptual mechanical designs presented here, preliminary assessments of weight and cost impacts were conducted.

***Modified Liner Concept***

The conceptual design of a modification to the nozzle liner to provide an $A_s/A_8$=1.1 is shown in Fig. 19. The JSF exhaust system features a perforated liner that is supported approximately 2.5 cm away from the duct wall. The function of the liner is to provide a thermal barrier to protect the exhaust duct from hot engine gases during after-burning. The gap between the liner and the exhaust duct forms a passage containing cooling air from the engine fan stream. The liner is perforated to allow a continuous flow of cooling air to pass through and protect it from hot engine core gases. In the baseline design, the liner terminates just up-stream of the throat. Air exiting from the trailing edge of the liner provides a cooling film to protect the nozzle divergent flaps.

The proposed design incorporates a turned-up lip at the trailing edge of the liner. As shown in Fig. 19, this modified liner provides the step geometry of $A_s/A_8$=1.1 required to induce separation at hover. Due to the geometry of the convergent flaps, the liner trailing edge is retracted upstream of the throat at cruise conditions, and does not present a step in the divergent section of the nozzle.

This preliminary design study indicates that the modified liner concept appears to be mechanically feasible, and easy to implement. A preliminary assessment of this design change anticipates no appreciable weight or cost impact from this benign change to the nozzle liner design. However, the liner provides critical cooling flow to the nozzle during after-burning conditions so modifications to the current design need to be fully assessed from a heat transfer perspective.

***Offset Hinge Concept***

The second concept studied utilizes an offset hinge between the trailing edge of the convergent flap and the leading edge of the divergent flap. In the baseline nozzle design, a simple hinge is used in this location, allowing the trailing edge of the convergent flap to remain in contact with the trailing edge of the divergent flap forming a continuous flow-path as the nozzle is articulated.

The proposed modification provides an offset hinge as shown in Fig. 20. The hinge point is located radially outward and aft of the trailing edge of the convergent flap. This hinge is designed to align the trailing edge of the convergent flap with the leading edge of the divergent flap at the cruise condition to provide a continuous flow-path. At the hover condition, however, the hinge geometry causes the divergent flap leading edge to move radially outward from the trailing edge of the convergent flap creating a step of $A_s/A_8$ = 1.1.

This preliminary design study indicates that the offset hinge concept appears to be mechanically feasible, and easy to implement. The offset hinge requires additional structure in the form of brackets to support the hinge point at the new location offset from the main flap structure. The hinge and offset bracket mechanism can be accommodated within the envelope of the current nozzle without any mechanical interference. A preliminary estimate of this design change anticipates a mass increase of less than 10 kg for hinge support brackets required since the hinge point is not located directly on the flap structure. No significant production cost impact is expected from this design change.

## Conclusions and Recommendations

The ACE propulsion nozzle concept featuring a boundary layer control step provides a thrust increase of approximately 2.5 percent relative to the baseline at the JSF hover condition. The design parameters and performance predictions for the step configuration were developed using numerical analysis and verified through subscale model testing. This study defines the fundamental geometric parameters for a successful step concept, and provides preliminary designs for incorporating the concept in the JSF nozzle. In addition, the extensive CFD analysis matrix yields results that may be generalized to other over-expanded internal transonic flows.

The results of this study indicate that a minimum step size of $A_s/A_8$ = 1.1 will induce flow separation and relieves over-expansion loss at the hover condition of NPR = 2 for the JSF nozzle with $A_9/A_8$ = 1.3 resulting in a 2.5 percent improvement in thrust. A larger step sizes of $A_s/A_8$ = 1.2 produce undesirable step drag at higher NPR conditions.

The results indicate that for a given value of $A_9/A_8$, increasing step size will induce separation at higher NPR. For a nozzle with $A_9/A_8$ = 1.3, a step size of $A_s/A_8$ = 1.1 will induce separation at NPR < 2, and the flow will reattach at NPR = 2.3 and above. With a step size of $A_s/A_8$ = 1.2, the separation occurs at a higher value of NPR = 2.3. The NPR at which separation occurs is also a function of $A_9/A_8$, with separation onset occurring at higher NPR with increasing $A_9/A_8$. For a nozzle with $A_9/A_8$ = 1.5 and $A_s/A_8$ = 1.1, the onset of separation occurs at NPR = 2.5 compared with NPR = 2.3 for the $A_9/A_8$ = 1.3, $A_s/A_8$ = 1.1 case.


### Acknowledgements

The authors acknowledge the support of Lockheed Martin Aeronautics Company (LMAC) for this study. They also are indebted to Brad Glass, John Richey and Brant Ginn of LMAC for their technical expertise in CFD analysis, model design and test data analysis respectively.


### References


1. Lu, F.K. and Terrier, D.A., "Performance Analysis of STOVL Aircraft Nozzle in Hover," AIAA Paper 2003–0184.
2. Carlson, J.R., Pao, S.P. and Abdol-Hamid, K.S., "Computational Analysis of Vented Supersonic Exhaust Nozzles Using a Multiblock/Multizone Strategy," *Journal of Propulsion and Power*, 1993, Vol. 9, No.6, pp. 834–839.
3. Leavitt, L.D. and Bangert, L.S., "Performance Characteristics of Axisymmetric Convergent-Divergent Exhaust Nozzles with Longitudinal Slots in the Divergent Flaps," NASA Technical Paper 2013, 1982.
4. Miller, D., Yagle, P. and Hamstra, J., "Fluidic Throat Skewing for Thrust Vectoring in Fixed-Geometry Nozzles," AIAA 99–0365, 1999.
5. Vakili, A.; Sauerwein, S.; Miller, D., "Pulsed Injection Applied to Nozzle Internal Flow Control," AIAA 99–1002, 1999.
6. Der, J., "Improved Methods of Characterizing Ejector Pumping Performance," *Journal of Propulsion and Power*, 1989, Vol. 7, No. 3, pp. 412–419.
7. Greathouse, W.K. and Beale, W.T., "Performance Characteristics of Several Divergent Shroud Ejectors," NACA RM E55G21a, September 1955.
8. Abu-Hijleh, B. and Samimy, M., "An Experimental Study of a Reattaching Supersonic Shear Layer," AIAA Paper 89–1801, 1989.
9. Hama, F.R., "Experimental Studies on the Lip Shock," AIAA Journal, Vol. 6, No. 2, pp. 212–219, 1968.
10. Kochendorfer, F.D. and Rousso, M.D., "Performance Characteristics of Aircraft Cooling Ejectors Having Short Cylindrical Shrouds," NACA RM E51E01, 1951.
11. Luffy, R.J. and Hamed, A., "A Study on the Impact of Shroud Geometry on Ejector Pumping Performance," AIAA Paper 92–3260, 1992.


**Table 1. Nozzle Conditions at Key JSF Mission Points**

| Mission Point | NPR | Temperature |
|---|---|---|
| Cruise | 3–4 | 780 K |
| Acceleration | 6–8 | 2,000 K |
| Hover | 2 | 780 K |

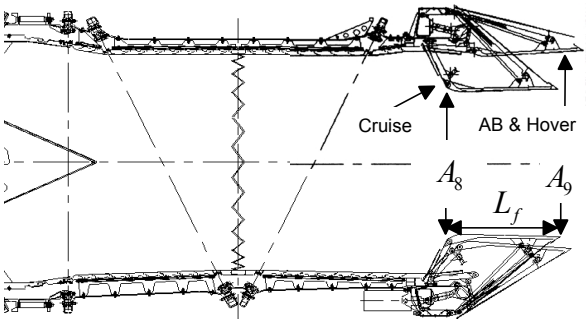


**Figure 1. JSF convergent-divergent nozzle.**

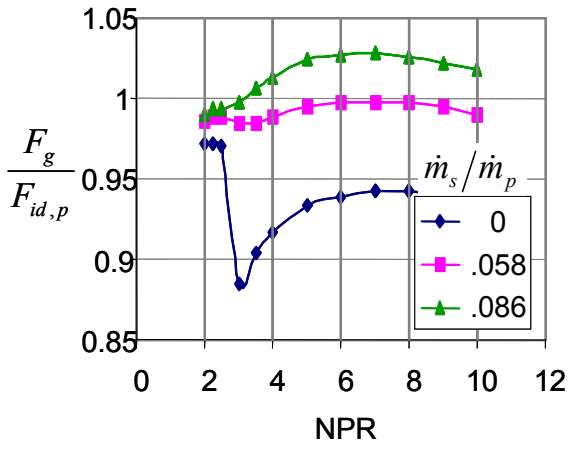


**Figure 2. Example of ejector performance ($A_9/A_8$ = 1.5, $A_s/A_8$ = 1.44).**[7]

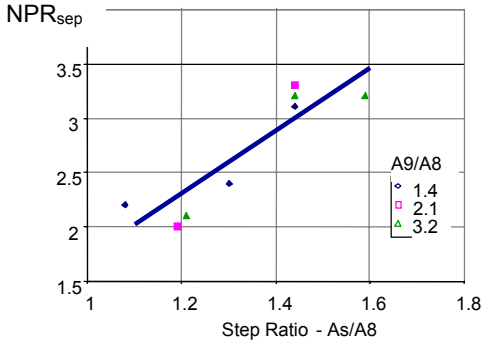


**Figure 3. Minimum step size for separation correlation (line drawn as visual aid).**

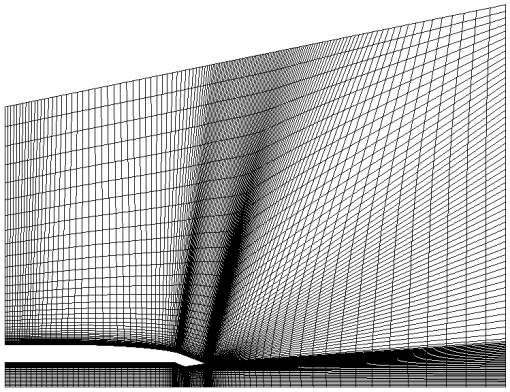

**Figure 4. Grid for $A_9/A_8$ = 1.3, the baseline configuration.**

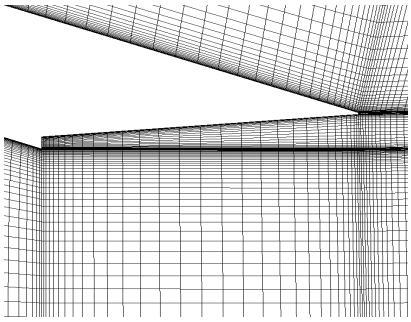

**Figure 5. Grid for $A_9/A_8$ = 1.3, $A_s/A_8$ = 1.1 configuration.**

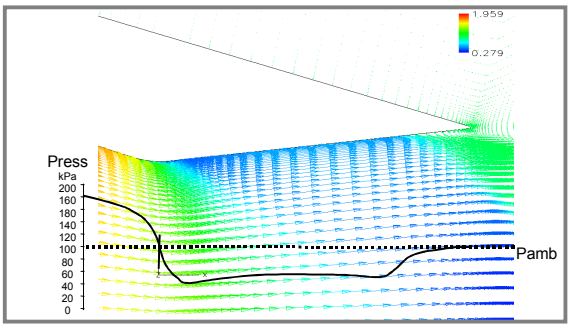


**Figure 6. CFD result for $A_9/A_8$ = 1.3, baseline nozzle, NPR = 2.**

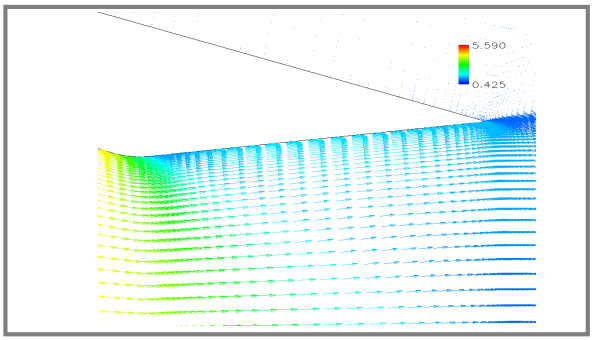


**Figure 7. CFD result for $A_9/A_8$ = 1.3, baseline nozzle, NPR = 6.**

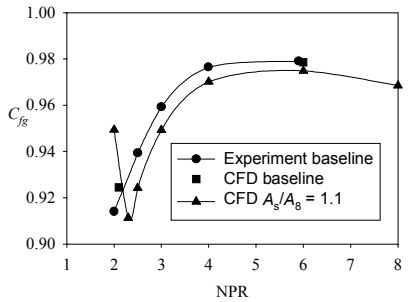


**Figure 8. Comparison of numerical and experimental values of gross thrust coefficient (lines for visual aid).**

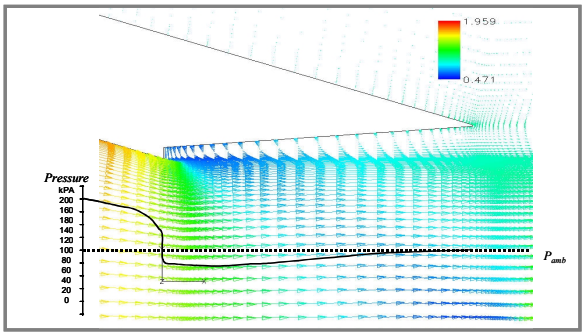


**Figure 9. CFD result for $A_9/A_8$ = 1.3, $A_s/A_8$ = 1.1, NPR = 2.**

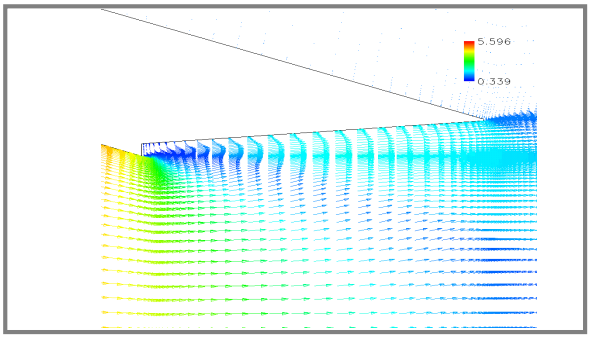


**Figure 10. CFD result for $A_9/A_8$ = 1.3, $A_s/A_8$ = 1.1, NPR = 6.**

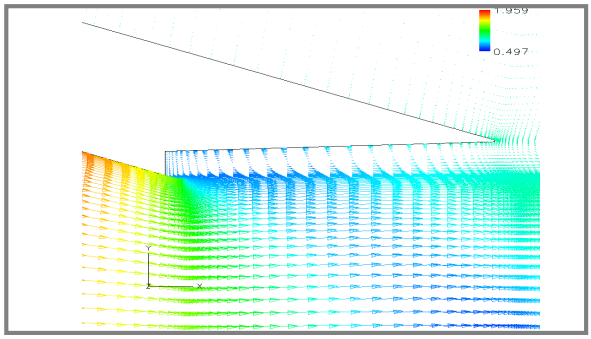


**Figure 11. CFD result for $A_9/A_8$ = 1.3, $A_s/A_8$ = 1.2, NPR = 2.**

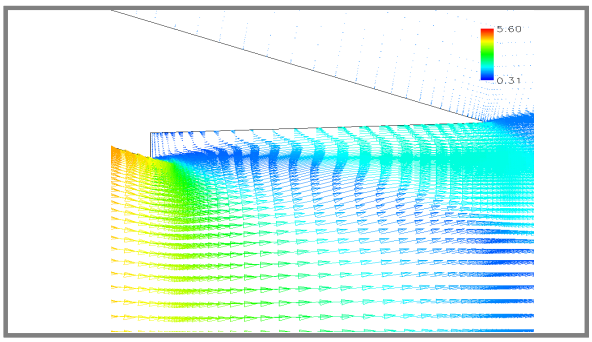


**Figure 12. CFD result for $A_9/A_8$ = 1.3, $A_s/A_8$ = 1.2, NPR = 6.**

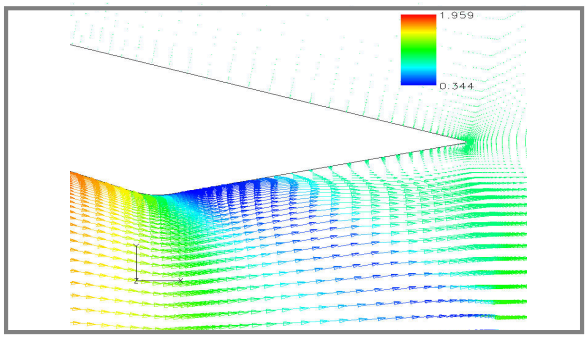


**Figure 13. CFD result for $A_9/A_8$ = 1.5, baseline nozzle, NPR = 2.**

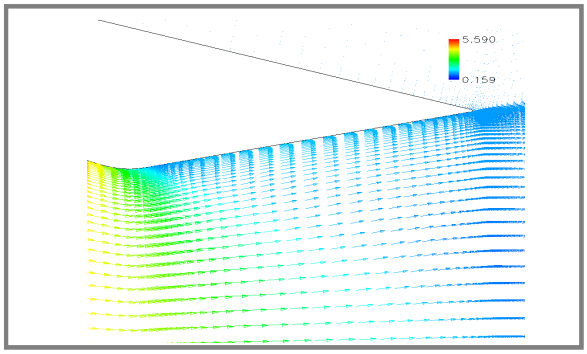


**Figure 14. CFD result for $A_9/A_8$ = 1.5, baseline nozzle, NPR = 6.**

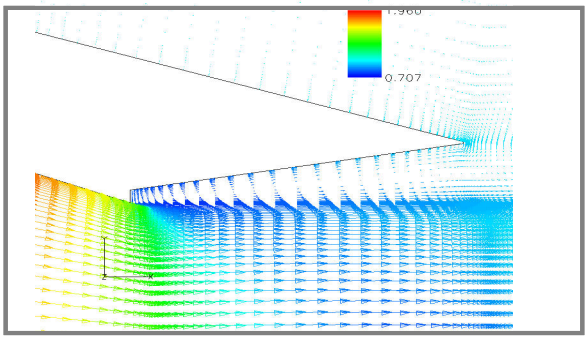


**Figure 15. CFD result for $A_9/A_8$ =1.5, $A_s/A_8$ = 1.1, NPR = 2.**

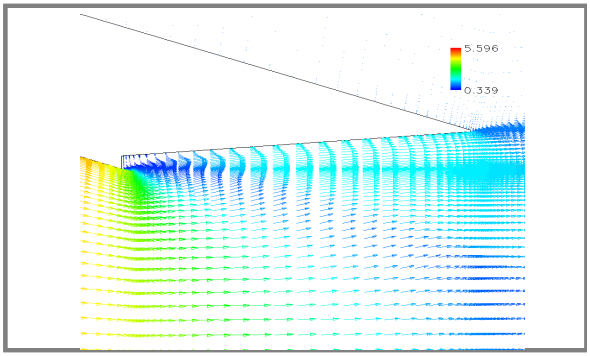


**Figure 16. CFD result for $A_9/A_8$ =1.5, $A_s/A_8$ = 1.1, NPR = 6.**

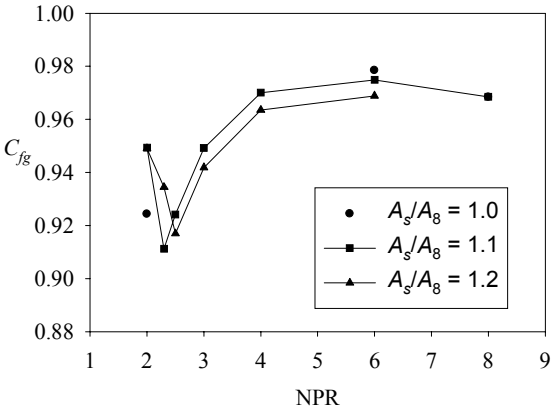


**a. $A_9/A_8$ = 1.3,**

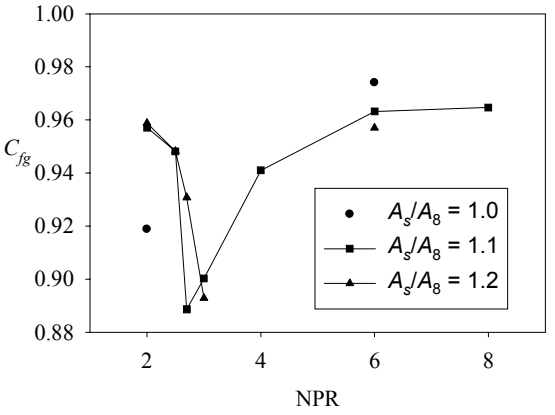


**b. $A_9/A_8$ = 1.5,**

**Figure 17. Gross thrust coefficients for various nozzle configurations (lines for visual aid).**

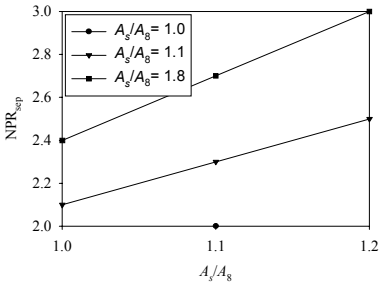


**a. Separation NPR.**

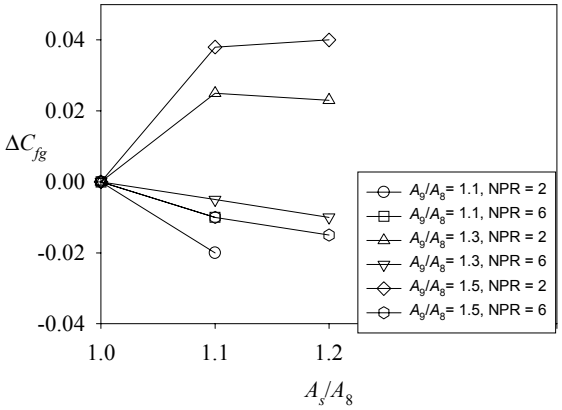


**b. Gross thrust coefficient.**

**Figure 18. Effect of step size on nozzle performance (lines for visual aid).**

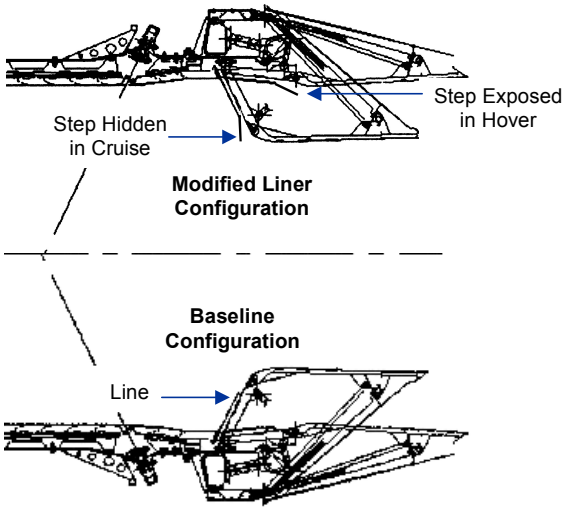


**Figure 19. Preliminary mechanical design of modified liner concept.**

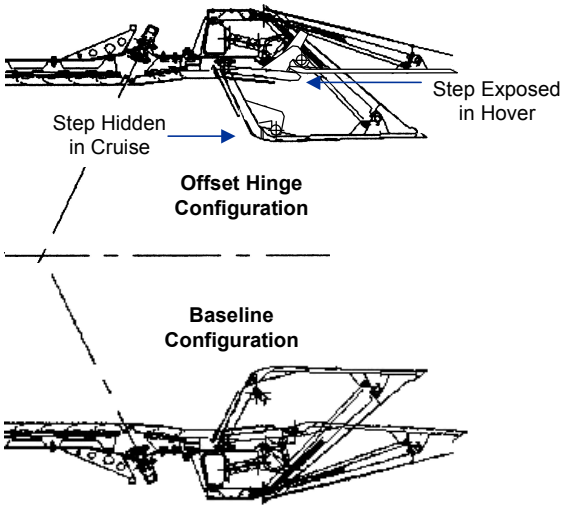


**Figure 20. Preliminary mechanical design of offset hinge concept.**